International Journal of Power Electronics and Drive Systems (IJPEDS)
Vol. 15, No. 2, June 2024, pp. 858~873
ISSN: 2088-8694, DOI: 10.11591/ijpeds.v15.i2.pp858-873

Performance of grid-connected photovoltaic systems in Northern and Southern Hemispheres under equatorial climate

Yang Ilya Akila Abdul Rahim[1], Hedzlin Zainuddin[1,2], Eko Adhi Setiawan[3], Alfian Ferdiansyah Madsuha[3,4], Mohamad Zhafran Hussin[5], Shahril Irwan Sulaiman[6], Siti Nor Nadhirah Ibrahim[1]

[1]Faculty of Applied Sciences, Universiti Teknologi MARA (UiTM) Shah Alam, Selangor, Malaysia
[2]Solar Photovoltaic Energy Conversion Technology and Research Application (SPECTRA), Universiti Teknologi MARA (UiTM) Shah Alam, Selangor, Malaysia
[3]Tropical Renewable Energy Center, Faculty of Engineering, Universitas Indonesia, Depok, Indonesia
[4]Department of Metallurgical and Materials Engineering, Faculty of Engineering, Universitas Indonesia, Depok, Indonesia
[5]School of Electrical Engineering, College of Engineering, Universiti Teknologi MARA (UiTM) Cawangan, Johor, Malaysia
[6]School of Electrical Engineering, College of Engineering, Universiti Teknologi MARA (UiTM) Shah Alam, Selangor, Malaysia

Article Info

Article history:

Received Jul 25, 2023
Revised Dec 22, 2024
Accepted Jan 9, 2024

Keywords:

Equatorial climate
Grid-connected (GC)
Photovoltaic (PV)
PVsyst
System performance

ABSTRACT

This work studied the actual and simulated technical performance between two grid-connected photovoltaic (GCPV) systems representing opposite latitudes. The system with a capacity of 5.4 kW_p installed in Kelantan, Malaysia represents the northern equator, and the 183.6 kW_p system installed in Cikarang, Indonesia, denotes the southern equator. The performance was simulated using PVsyst software, which included the energy output (E_{out}), reference yield (Y_r), final yield (Y_f), performance ratio (PR), and capacity factor (CF). The mean bias error (MBE) between the actual and simulated technical performance were as follows; for system A, the yearly MBE for the E_{out}, Y_r, Y_f, PR, and CF were -0.4%, 17.1%, -1.4%, -15.8%, and 1.4%, respectively, and for system B, the E_{out}, Y_r, Y_f, PR, and CF values were 9.80%, 18.3%, 10.0%, -7.2%, and 10.0% respectively. The results have proven that PVsyst has successfully simulated the yearly E_{out}, Y_f and CF for both systems including PR, for system B, with MBE less than 10%. However, it is noteworthy to highlight that PVsyst significantly overestimated the Y_r of both systems up to 18.3% and conversely underestimated the PR for system A by 15.8%, which highly likely caused by the Meteonorm imported weather data.

Corresponding Author:

Hedzlin Binti Zainuddin
Solar Photovoltaic Energy Conversion Technology and Research Application (SPECTRA)
Universiti Teknologi MARA (UiTM) Shah Alam
Selangor, Malaysia
Email: hedzl506@uitm.edu.my

1. INTRODUCTION

Renewable energy sources, such as solar, wind, hydro, geothermal, and biomass, are sustainable energy sources that have become popular in the modern world. Solar energy is one of the most essential and fundamental renewable energy sources because it is abundant and is used to generate electricity in most parts of the world [1]. Photovoltaic (PV) systems are practical and competitive options for transitioning to sustainable energy systems. Globally, the energy produced by PV systems has increased, reaching 760 GW in 2020 [2]. The trend analyses show an exponential increase in the total installed capacity, along with increased efficiency and decreased system prices, which piques the curiosity of more people globally and draws new stakeholders to a range of markets [3].

Researchers worldwide have studied the performance of PV systems from the module level to the utility-scale in various climates. The system requires International Electrotechnical Commission (IEC) 61724 International Performance Monitoring to analyze the performance of several installations located and operating in various climates. Several technical performance parameters were recommended by the IEC through the IEC61724 standard to identify the best performers across the PV system. The performance parameters included the final yield (Y_f), reference yield (Y_r), and performance ratio (PR). These performance indices allow cross-comparison between several PV systems under different climatic conditions [4]. The technical performance evaluated using in-field monitoring data is also helpful for PV system designers, installers, researchers, and end users because they serve as a performance benchmark for component manufacturers [5]. The performance ratio for a 2.5 kW_p installation in the Saharan environment in Algeria ranged from 66.66% to 85.93%. This broad interval is due to the significant temperature difference between seasons [6].

Anang *et al*. [7] performed a technical performance analysis of a 7.8 kW_p grid-connected PV (GCPV) system rooftop in Kuala Terengganu, Malaysia. In addition, they conducted a performance analysis using the IEC61724 standard. According to the performance analysis, the best PR, value was 75.72%, and the average loss was 1.68 kWh/kW_p/day. The annual capacity factor (CF) and overall system efficiency ranged from 13% to 16% and 10% to 12%, respectively. Furthermore, in Daher *et al.* [8], the PR for a 302.4 kW_p installation operating in a dusty desert maritime climate ranged between 75% and 90%. The average daily array yield and final monthly yield were 5.1 kWh/kW_p and 4.7 kWh/kW_p, respectively. The average performance ratios for PV arrays and the global grid-connected system were 90% and 84%, respectively, corresponding to a monthly average of daily PV modules and system efficiencies of 12.68% and 11.75%.

Lima *et al*. [9] reported another example of the standard application in the northeast region of Brazil, monitored from June 2013 to May 2014. The performance analysis of a 2.2 kW_p PV system installed at the State University of Ceará, Fortaleza, revealed a suitable performance with an annual energy yield, an average daily reference, an array, and final yields of 1685.5 kWh/kW_p, 5.6 kWh/kW_p, 4.9 kWh/kW_p, and 4.6 kWh/kW_p respectively. Moreover, a 600 W_p PV system connected to the 220 V network of the Facultad de Ciencias Exactas building in Corrientes, Argentina, demonstrated a PR of 65% to 75% during the first ten months of operation between January 2011 and December 2012. This was consistent with those reported in other studies, specifically for systems installed on facades. However, the PR has fallen below 65% owing to network parameter instabilities since November 2011 [10].

The performance of a newly installed 281 kW_p first GCPV solar farm in Lesotho, a country located in Southern Africa, was evaluated using IEC Standard 61724 parameters. The results demonstrated good performance, with a weighted PR of 70% compared with the global average of 70% to 80% for adequately performing PV farms [11]. It is critical to compare the performance parameters deduced from the actual data with the simulated performance to evaluate the accuracy of the software for future installations. Most frequently, the PV system performance using commercial software is performed during the project planning stage, particularly during the preparation stage [12]. Various PV simulation software packages employ various power models, databases, irradiance decomposition methods, and other features. Several simulation software packages, including HOMER, PV*SOL, RETScreen, and PVsyst, were used for designing PV systems. PVsyst is a design tool that optimizes grid-connected, standalone, and pumping PV systems based on their location on the map. The tool also depends on the consumer's electricity profile and demand. It also provides financial visibility for the designed project, measuring environmental impacts in tons. The losses in the system can also be calculated [13].

Silva *et al*. [14] modelled a PV plant at the University of Campinas in Campinas, Brazil, using HOMER, PV*SOL, and PVsyst. According to their research, the value predicted by HOMER was under-predicted, PV*SOL was over-predicted, and PVsyst predicted the closest to the plant's measured values. These findings led to the recommendation of the PVsyst software for large-scale installations. Moreover, several studies have also applied PVsyst to estimate the GCPV system technical performance in equatorial regions. Tarigan et al. [15] simulated the techno-economic analysis of a GCPV system in Surabaya, Indonesia, using PVsyst and RETscreen. The technical analysis using PVsyst in the study shows that a 1 kW_p GCPV system simulation managed to generate 1.3 MWh electricity per year, and the performance ratio for the system was approximately 73%. The study also found that the highest losses resulted from the array and inverter losses, which were 22% and 4.4%, respectively.

Abdullah *et al*. [16] used the PVsyst software to perform a performance analysis of different types of PV modules for a 3 kW residential rooftop GCPV system in Selangor, Malaysia. Monocrystalline, polycrystalline and heterojunction with intrinsic thin layer (HIT) PV panels were used for comparative analysis in a 3.12 kW rooftop PV system. The PV module was analyzed using its exact location, weather, orientation, and losses to ensure a fair comparison. Polycrystalline produced the most energy to the grid, with 4046.9 kWh, followed by mono (3737.2 kWh) and HIT (3810.3 kWh). Although polycrystalline produced more solar energy for the grid, the annual PR of the HIT panel was 81%, compared to 79% for polycrystalline and 79.5% for monocrystalline. The study concluded that the performance of HIT PV modules was superior to that of monocrystalline and polycrystalline -type PV modules owing to fewer losses and higher output [15].

In addition, Mansur *et al*. [17] used PVsyst to design and simulate a 4.0 kW_p solar PV system for a residential place under the Net Energy Metering (NEM) framework in Changlun, Malaysia. Based on the techno-economic study, the energy generated was 5704.4 kWh per year, with 9.7% used by the home load and the remaining 90.3% sent to the grid. The annual performance ratio was 79.6%, with an average daily energy production of 3.91 kWh/kW_p. This NEM design setup is estimated to generate a profit of RM 1187 per year for residential customers while nearly reducing 4.0 tons of CO_2 emissions into the atmosphere.

Moreover, Hussain *et al.* [18] used the PVsyst software to perform a techno-economic analysis of commercial-size grid-connected rooftop solar PV systems under the NEM 3.0 scheme in Malaysia. At a net capacity factor (CF) of 18%, the system is expected to generate approximately 510 MWh of energy in the first year of operation. The annual degradation factors were 2.5% in the first year and 0.7% in the second year. The average PR was 0.803. The study found that temperature was responsible for the most significant losses, accounting for 7.77% of the total. In contrast, inverter losses were only 1.47%, which aligns with component manufacturing data This study also includes a financial analysis to assess the system's profitability, focusing on commercial buildings under the NEM 3.0 and resulting in an 8.4-year return on investment (ROI).

The GCPV system generates the most significant amount of energy. Consequently, the performance of PV systems is a parameter that determines their efficiency. This study aimed to analyze the technical performance of two case studies of GCPV systems in the northern and southern hemispheres of the equatorial climate. The technical performance analysis was simulated using the PVsyst software and compared with the actual technical performance analysis as the benchmark. Nevertheless, this study will be limited to five technical performance parameters based on the data availability: E_{out} Y_f, Y_r, PR, and CF. Because most of the performance study was conducted within specific locations or geographical boundaries, this study was unique in comparing the technical performance of GCPV systems in different geographical boundaries yet different hemispheres of a tropical region, which are 6 degrees north and south of the equatorial line.

2. METHOD

The framework of this study is illustrated in Figure 1. The primary step was to compare the technical performances of the actual and simulated systems. This method framework will be explained in four sections, which are data compilation, PVsyst simulation, technical performance analysis using IEC61724:2021 and technical performances comparison for two GCPV sites. These two sites were selected because they are located at almost the same latitude but in different hemispheres. The systems were designated as systems A and B. System A is a 5.39 kW_p system in Kelantan, Malaysia, and system B is a 183.6 kW_p system located in Cikarang, Indonesia.

Section 2.2 discusses how these parameters were then used to simulate the system using the PVsyst software. To estimate the technical performance of the selected systems in the PVsyst software, the simulation design results must follow specifications according to the existing system: i) the model and specifications of the PV module and inverter used must be the same as the existing system; ii) the configuration of the array and inverter must be in line with the actual system; and iii) the configuration must fulfil the energy required for both systems. Then, in section 2.3, the technical performance of the existing systems is calculated based on IEC61724 standard, and lastly in section 2.4, the results of both methods are compared using error metric. All of these sections will be thoroughly discussed in the next section.

2.1. Data compilation

This section compiles the three types of information for systems A and B, as shown in Figure 2. The information compiled included system information, component information, and measured data from every 5 min interval. The system information and component information will later be used in section 2.2, while the measured data will be used in section 2.3.

System A is a 5.39 kW_p GCPV system installed on the rooftop of a mosque in Kelantan, Malaysia. The system is located at 6.13°N and 102.26°E; it was installed by the end of 2014. The system consisted of 22 silicon PV modules with 245 W_p each. The 22 PV modules were arranged in two parallel strings, and the PV arrays were inclined at 10° facing the southwest. The strings are connected to PVI-5000/6000-TL-OUTD which is a 5-kW inverter which feed directly into the grid.

Located at 6.29°S and 107.10°E, Cikarang, Indonesia, system B is a 183.6 kW_p GCPV system on a factory's rooftop; it was installed by the end of 2020. The system consists of 540 silicon PV modules, each with a maximum power of 340 W_p. The 540 PV modules are arranged in 27 parallel strings, each consisting of 20 PV modules. The PV arrays are inclined at 7°, facing south. Moreover, the strings are connected to Solid

Q-50 which is a 50-kW inverter which feed directly into the grid. A summary of the system information, PV module, and inverter specifications of both systems is provided in Tables 1-3, respectively. The measured data consisted of three parameters: in-plane irradiance (H_i), module temperature (T_m), and AC power (P_{ac}). The data were extracted from the data logger with 5 min logging intervals, in compliance with the requirements of the international standard IEC61724.

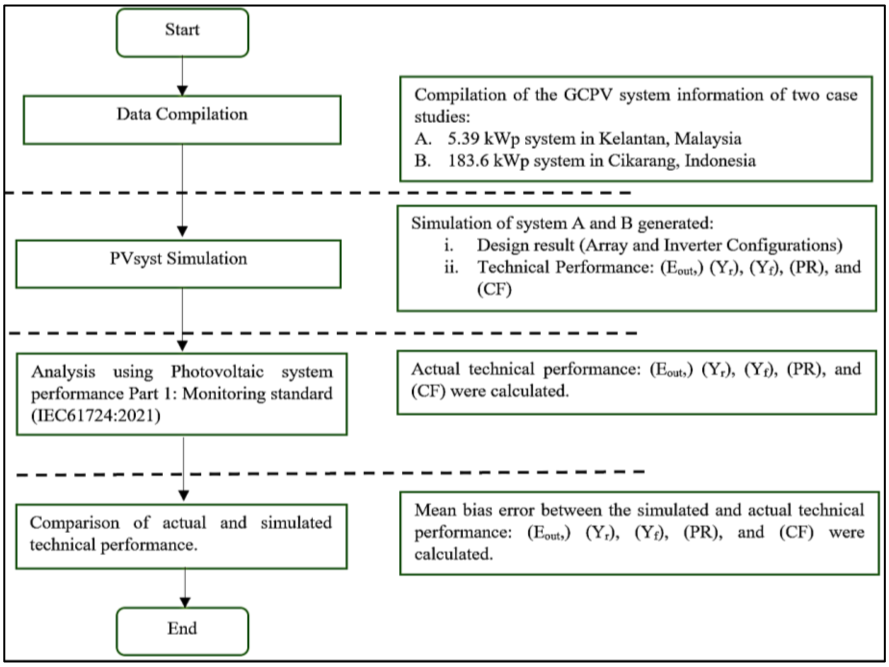

Figure 1. Framework of the study

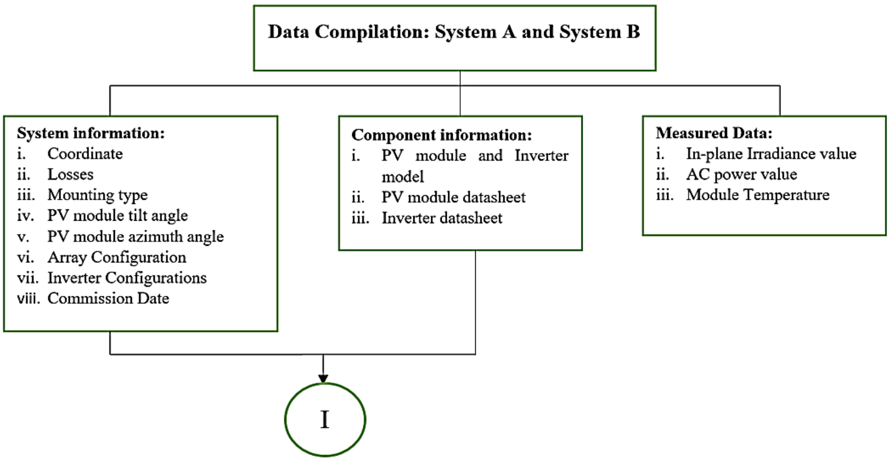

Figure 2. Data compilation of systems A and B (I continued to Figure 3)

Table 1. General information for systems A and B

Parameter/System	A	B
Location	Kelantan, Malaysia	Cikarang, Indonesia
Site coordinates	6.13°N, 102.26°E	6.29°S, 107.10°E
Mounting	Free - Standing	Retrofitted
PV array	5.39	183.6
Array configuration	1×11	27×20
Inverter configuration	1×1	1×3
PV array tilt angle and orientation	10° facing southwest	7° facing south
Commission date	Dec-2014	Jan-2020

Table 2. PV module specification for systems A and B

System		A	B
Description	Unit		
Brand		Hanhwa	Trina solar
Model	-	Hanhwa- Q Cell Q-Pro-G3	TallMax TSM_DD4A (II)
Type of PV technology		Polycrystalline	Polycrystalline
Maximum power at STC	W_p	245	340
Open circuit voltage	V	37.56	46.2
Short circuit current	A	8.85	9.50
Maximum power voltage	V	29.73	38.2
Maximum power current	A	8.32	8.90
Temperature coefficient of voltage	$\%°C^{-1}$	- 0.33	- 0.29
Temperature coefficient of current	$\%°C^{-1}$	0.04	0.05
Temperature coefficient of power	$\%°C^{-1}$	-0.43	- 0.39

Table 3. Inverter specification for systems A and B

System		A	B
Description	Unit		
Brand		ABB	SMA
Model	-	PVI-5000/6000-TL-OUTD	Solid Q-50
No. of inverter	-	1	3
Nominal power	kW	5	50
Maximum voltage	V	600	1000
Range of minimum and maximum MPPT voltage	V	150..530	200..950
Maximum AC	A	25	80
No. of MPPT	-	2	3
Inverter efficiency	%	97	>98

2.2. PVsyst simulation

The PVsyst software was used in this study to predict the performance indices and energy output of systems A and B. The designs of both systems must be simulated before determining the performance indices. The steps applied for designing both systems using PVsyst are illustrated in Figure 3 [19]. The PVsyst simulation inputs are categorized into two sections: project information and simulation information.

Project information consists of site details such as the project's name and coordinates. From the coordinates, the meteorological data of the selected systems were generated using the Meteonorm 8.0 database. The Meteonorm 8.0 database was selected based on a previous study that simulated the GCPV system using the PVsyst software [20]–[24].

Next, the simulation information consists of the systems' main components, orientation, and losses. The PV module and inverter used are based on the installed system specifications in Tables 2 and 3. Because some of the PV module and inverter models are not listed in the PVsyst database, the specifications of these components were inserted manually into the PVsyst software. Then, the reference module temperature was applied such as most similar studies which a minimum of 20 °C and a maximum of 75 °C [25]–[27].

Then all these data were then simulated to obtain the design result. PVsyst processes the project information and the simulation information to generate the simulated GCPV design result, which comprises the PV array and inverter configurations. Then, the system losses, which consist of thermal losses, ohmic losses, light-induced degradation (LID) losses, soiling losses, incidence angle modifier (IAM) losses, auxiliary losses, aging losses, unavailability, and spectral collection, were inserted to enable the PVsyst software to simulate the design and performance results. The performance results included technical, economical, and environmental factors. However, owing to limitations in available information, this study is limited to analyzing the design result (array and inverter configuration) and technical performance, including E_{out},Y_f, Y_r, PR, and CF.

2.2.1. Loss in PVsyst

Various losses are involved in generating the energy output from a PV system. These include two types of losses: thermal capture and miscellaneous capture. Thermal capture losses are caused by cell temperatures higher than 25 °C. Miscellaneous capture losses are due to low irradiance, shading, dust accumulation on modules, mismatch, and wiring. In this study, the approach of determining the appropriate values of losses was prioritized using the values provided by the PV module and inverter manufacturer's datasheet, followed by values used in several works of literature in similar studies, and finally default values by the PVsyst software. The PVsyst simulation included 12 losses, as listed in Table 4.

In this study, two losses were taken from the manufacturer's datasheet: the losses by aging (k_{age}) and the losses from the inverter (inv_{loss}). System A has been operating since late 2014, approximately five years.

Thus, k_{age} was simulated based on the power degradation information from the datasheet. However, system B has no losses due to aging because it is a newly installed system. For inv_{loss}, the values were obtained from the inverter datasheet based on the declared maximum efficiency. The other two losses obtained from the literature [28] are the losses due to dirt (k_{dirt}) and wiring ($cable_{loss}$). k_{dirt} was set to be 3% and $cable_{loss}$ was as also set to 3% based on [28] and many similar case studies conducted by [29]–[32].

For the other four losses, namely, temperature losses (k_{temp}), mismatch losses (k_{mm}), LID, and IAM, the values applied were the default values provided by the PVsyst software. Notably, the thermal loss factor provided by PVsyst differs based on the mounting type of the array, which is 29 W/m^{2}K for free-standing mounting and 20 W/m^{2}K for retrofitted mounting. The temperature losses varied between the two systems, with system A experiencing an 8.86% loss as it was free-standing, while system B, which was retrofitted, had a 10.09% loss. The k_{shade} loss was neglected in both cases because there was no shading on either selected site. Finally. The losses due to auxiliaries, unavailability, and spectral correction were not included because they were irrelevant in both cases.

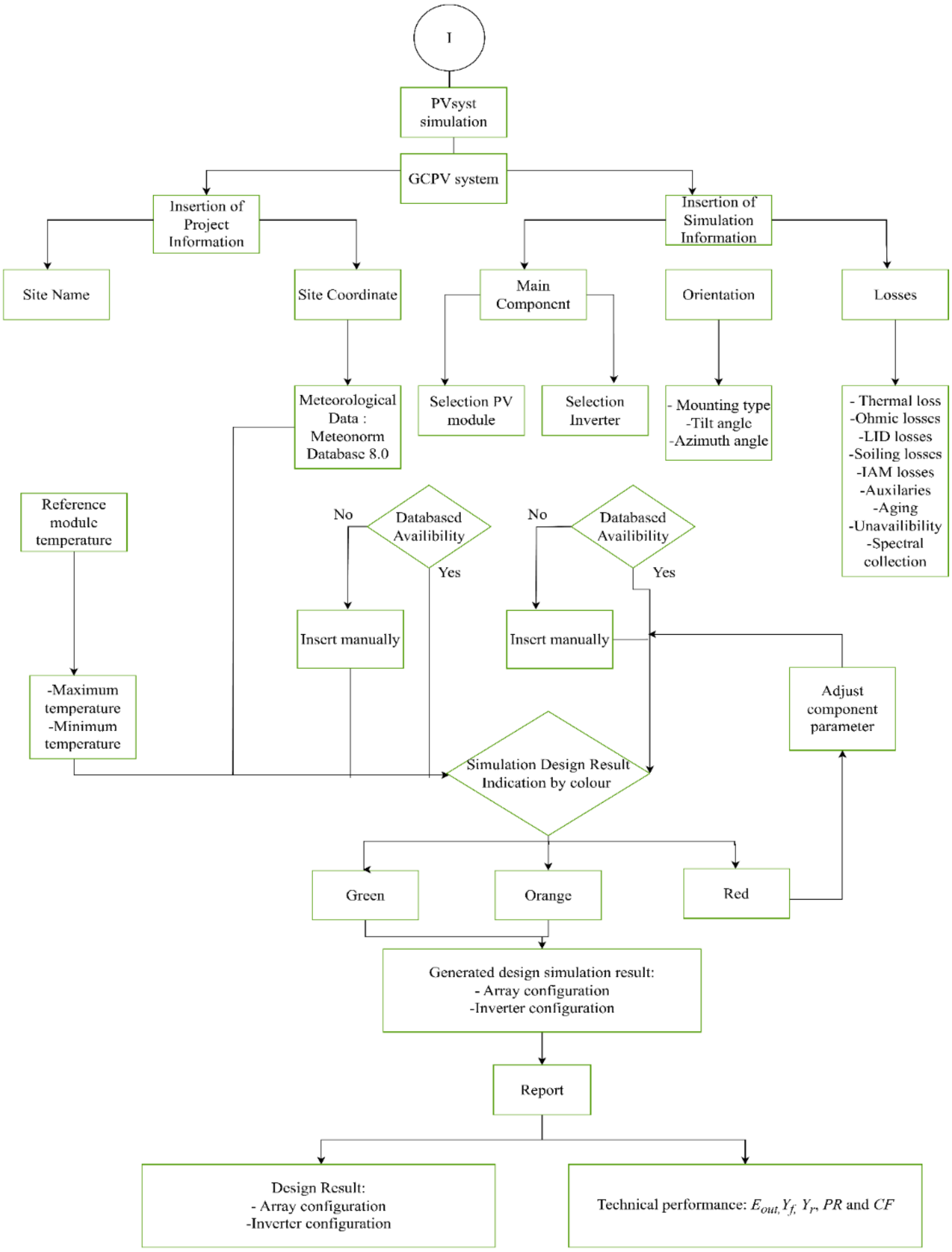

Figure 1. PVsyst simulation steps

Table 4. Losses used in PVsyst and their references

No	PVsyst Parameter	System A Value	System B Value	References: Manufacturer datasheet	References: PVsyst default	References: Other
1	k_{age} per year	0.60	0.55	√		
2	inv_{loss}	3	3	√		
3	k_{dirt}	3	3	√		√ [28]
4	$cable_{loss}$	3	3			√ [33]
5	k_{temp}	8.86	10.09		√ Thermal loss factor system A: 29 W/ m^2K Thermal loss factor system B: 20 W/ m^2K	
6	k_{mm}	2.21	2.10			
7	LID	3	3		√	
8	IAM Losses	2.39	3.08		√	
9	k_{shade}	0	0		√	
10	Auxiliaries	-	-	-	-	-
11	Unavailability	-	-			
12	Spectral correction	-	-			

2.3. Technical performance analysis

The International Electrotechnical Commission (IEC) has developed parameters that have been used in various studies to analyze the performance of the GCPV system [34]–[38]. Several performance parameters are listed in IEC61724, but this study is limited to performing an analysis of (1) reference yield (Y_r), (2) final yield (Y_f), (3) performance ratio (PR), and (4) capacity factor (CF) due to limitations in data availability.

The reference yield (Y_r) is the number of hours in which solar radiation must be at the reference irradiance levels to produce the same amount of incident solar energy observed during the reporting period when the utility grid or local load was available. The Y_r in (1) of a monofacial PV system can be calculated by dividing the total front-side in-plane irradiation by the module's reference plane-of-array irradiance, which is expressed as (1) [39].

$$Y_r = \frac{H_i}{G_i} \tag{1}$$

The H_i is the total front-side in-plane irradiation, and G_i is the reference plane-of-array irradiance, which equals 1 kW/m^2. If the reporting period is equal to one day, then Y_r would be, in effect, the equivalent number of sun hours at the reference irradiance per day. The Y_f in (2) parameter was used to compare the energy output performance of PV systems in different geographical regions. This parameter is the ratio of the total energy generated by the system to the installed peak power of the PV array under rated conditions (STC), which is expressed as [39] (2).

$$Y_f = \frac{E_{out}}{P_0} \tag{2}$$

E_{out} is the AC energy generated of the entire PV system per rated kilowatt system per year. Moreover, E_{out} is known as E_{grid} inside PVsyst. Next, P_0 is the array power rating under the rated conditions (STC). Therefore, Y_f normalizes the energy produced with respect to the system size. PR in (3), is the quotient of the system's final yield to its reference yield and indicates the overall effect of losses on the system, which is expressed as (3) [39].

$$PR = \frac{Y_f}{Y_r} \tag{3}$$

Y_f is the final yield of the system and Y_r is the reference yield of the system. PR represents how close to ideal performance a PV system is under real-world operating conditions; moreover, it allows for the comparison of PV systems, regardless of tilt angle, area, orientation, or nominal capacity. However, as the temperature of the PV module increased, most PR values were higher in colder months than in warmer months, resulting in additional losses. After accounting for energy losses, PR represents the amount of available energy [22]. PR typically ranges from 0.6 to 0.8, depending on the location, solar irradiation, and weather conditions.

The annual CF in (4), is another performance parameter. This parameter represents the ratio of the annual energy output to the energy produced by the PV system if operated for 24 h per day at full rated power, which is expressed as (4).

$$CF = \frac{E_{out\_yearly}}{P_{PV\_rated} \times 365 \times 24} \times 100 \tag{4}$$

CF is affected by the location of the PV system, and the higher the CF, the better is the performance of the PV system [37].

2.4. Result validation using mean bias error (MBE)

MBE in (5) was the parameter used to assess the divergence between the simulated technical performance from the PVsyst and that measured from the GCPV system. Values near 0 are the best, negative values indicate the underestimation of simulated result from PVsyst and positive values indicate overestimation of simulated results [40]. It is expressed as (5).

$$\mathrm{MBE} = \frac{\text{simulated value} - \text{measured value}}{\text{measured value}} \times 100 \tag{5}$$

3. RESULTS AND DISCUSSION

This section is divided into three sections. Section 3.1 compares the actual and simulated irradiations for systems A and B. Then section 3.2 compares the actual and simulated technical performances of systems A and B. This comparison helps quantify the deviation of the simulated values from the actual values. Finally, section 3.3 is a comparison of the actual technical performance for systems A and B is presented to determine any significant difference in the technical performance for two GCPV systems located within the equatorial line but at different hemispheres. Nevertheless, it is very important to highlight that for system A, the available one-year actual data were for 2019. Meanwhile, the available one-year actual data for system B were for 2020.

3.1. Comparison of the actual and simulated in-plane irradiation for systems A and B

This study compares two sources of weather data: actual measured at the site and Meteonorm-derived long-term data (1985-2015) (PVsyst, 2022) for systems A and B. Figure 4(a) shows the comparison of monthly actual in-plane irradiation (H_{i_actual}) and simulated in-plane irradiation ($H_{i\_simulated}$) combined with the corresponding MBE for system A. The figure shows that the H_i values of the actual and simulation for system A show a similar trend, although the magnitude of the MBE was quite high. The Meteonorm-derived data consistently overpredicted the value of actual irradiation throughout the year. The MBE varied in the range of 11% to 32%. The highest MBE was in January, which was 31.9%. The highest H_i recorded was in March for both H_{i_actual} and $H_{i\_simulated}$, which were 168.8 kWh/m^2 and 187.6 kWh/m^{2,} respectively. The lowest H_i value was recorded in December for H_{i_actual} and $H_{i\_simulated}$, which were 103.4 kWh/m^2 and 118.0 kWh/m^2, respectively.

Figure 4(b) shows a comparison of H_{i_actual} and $H_{i\_simulated}$ combined with the corresponding MBE for system B. The trends of the actual and simulated H_i were not in good agreement, except for three months: January, September, and November. The figure shows that Meteonorm-derived data also consistently overpredicted the value of actual irradiation throughout the year. The MBE varied in the range of 8% to 49%. The highest MBE was in February, which was 48.9%. The highest H_{i_actual} was recorded in September with a value of 152.0 kWh/m^2, and in October for $H_{i\_simulated}$ with a value of 168.8 kWh/m^2. The lowest H_i value was recorded in February for H_{i_actual} and in January for $H_{i\_simulated}$, which was 92.5 kWh/m^2 and 119.0 kWh/m^2, respectively.

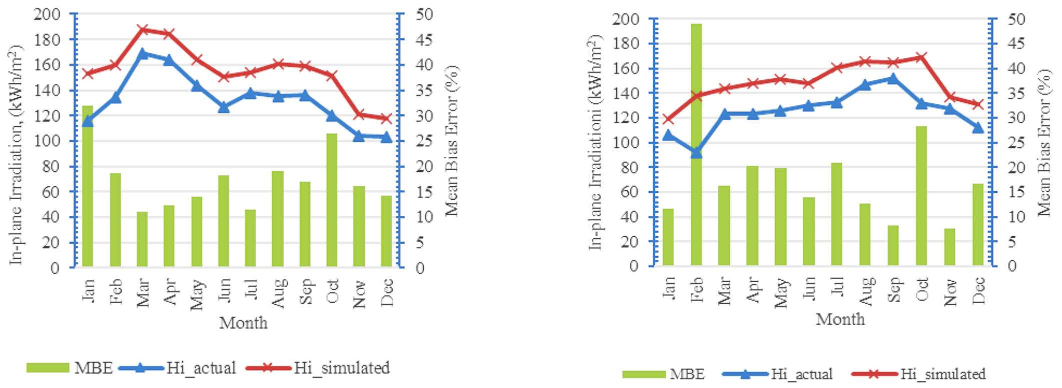

(a) (b)

Figure 4. Comparison between the value of the measured in-plane irradiation (H_{i_actual}) and the simulated in-plane irradiation ($H_{i\_simulated}$) for (a) system A and (b) system B

In summary, overprediction is expected from the $H_{i\_simulated}$ for both systems because Meteonorm provides long-term monthly data for a determined site created from the average statistical values over several years. Thus, it will rarely be the same as the real values for any particular month, which also occurred in a previous study conducted by Vidal *et al.* in 2020 [23]. Although a significant value exists in the monthly MBE of the H_i, the MBE for yearly H_i for both systems is considerable as they range between 17% and 18%. The highest value of H_{i_actual} recorded for system A is in line with the position of the sun since system A is located at the equatorial line, which is in March. Conversely, when the position of the sun is located further away from the equatorial line, which is in the tropic of Capricorn, Malaysians experience the northeast monsoon in November, which ends in February the following year; that is why the irradiation values in November and December are typically lower than those in the other months [41]. The irradiance ranged from 183 W/m^2 to 221 W/m^2, which is lower than that of months such as March and April, which ranged from 244 W/m^2 to 259 W/m^2 [30].

3.2. Comparison of the actual and simulated technical performance results of systems A and B

This section shows the comparison of the actual and simulated technical performances of systems A and B. The technical performance indices consist of E_{out}, Y_r, Y_f, PR, and CF which were presented on monthly and yearly basis. The monthly variations of the indices were illustrated in the form of a graph together with the corresponding MBE.

3.2.1. AC energy generated

Figure 5(a) shows a comparison of the monthly actual AC energy generated (E_{out_actual}) and simulated AC energy generated ($E_{out\_simulated}$) combined with the corresponding MBE for system A. The figure shows that the actual and simulated E_{out} trends are almost similar, with slight variations in January. The maximum E_{out} was recorded in March for both E_{out_actual} and $E_{out\_simulated}$, which were 765.3 kWh and 737.2 kWh, respectively, whereas the minimum E_{out} was recorded in December for both E_{out_actual} and $E_{out\_simulated}$, which were 485.2 kWh and 474.6 kWh. The figure shows that the $E_{out\_simulated}$ was very close to the actual values in the range of -0.4% to 5.6%, except for January, which was 11.9%.

Figure 5(b) shows the comparison of the monthly E_{out_actual} and $E_{out\_simulated}$ combined with the corresponding MBE for system B. The actual and simulated E_{out} trends show that they are not in good agreement, except for three months, that is, January, September, and November. For system B, the maximum E_{out_actual} was in September with a value of 22957 kWh, and the minimum was in February with a value of 14550.63 kWh. It is observed that significant differences exist between the actual and simulated values, except for January, March, September, and November, with MBE less than 5%. The figure shows that, on average, the PVsyst software significantly overpredicted the $E_{out\_simulated}$ in the range of 0.2% to 29%, where the highest was in February.

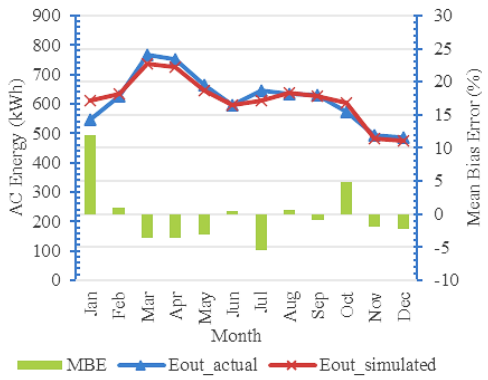

(a)

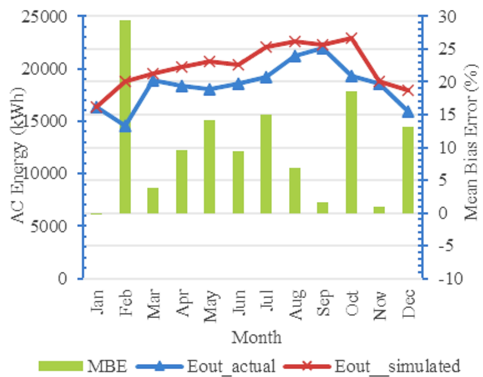

(b)

Figure 5. Comparison between the value of the actual energy output AC energy (E_{out_actual}) and the simulated energy output AC energy ($E_{out\_simulated}$) for (a) system A and (b) system B

The comparison shows that the maximum and minimum values of E_{out_actual} for both the systems are directly linked to the value of H_{i_actual} for each system. The highest H_{i_actual} for system A was in March, and that for system B was in September, which is in line with the highest E_{out_actual} recorded. The same is true for the minimum value of E_{out_actual} recorded. Therefore, the same conclusion can also be drawn for $E_{out\_simulated}$ by PVsyst, as it also shows the same trend as the E_{out_actual}. Although the MBE for monthly E_{out} for both systems is quite large, the yearly MBE only ranged between -0.4% to 9.8%. This MBE range can be considered small compared to a similar study conducted by Thotakura with a 30.64% deviation [42].

3.2.2. Reference yield

Figure 6(a) shows the comparison of the monthly actual reference yield (Y_{r_actual}) and simulated reference yield ($Y_{r\_simulated}$) combined with the corresponding MBE for system A. The figure shows that the actual and simulated Y_r values exhibit a similar trend. The highest Y_{r_actual} was recorded in March, with a value of 168.8 kWh/kW$_p$, whereas the lowest was recorded in December, with a value of 103.4 kWh/kW$_p$. The figure shows $Y_{r\_simulated}$ was over-predicted by PVsyst, with the MBE varying in the range of 11% to 32%. The highest MBE was recorded in January with 32%.

Figure 6(b) shows a monthly comparison of Y_{r_actual} and $Y_{r\_simulated}$ combined with the corresponding MBE for system B. The trends of the actual and simulated H_i are not in good agreement, except for the three months: January, September, and November. The highest Y_{r_actual} was recorded in September (151.6 kWh/kW), while the lowest Y_{r_actual} was recorded in February (92.5 kWh/kW$_p$). The Figure shows that $Y_{r\_simulated}$ was overestimated for the entire year. The MBE varied in the range of 7.5% to 54%. The highest MBE was recorded in February, which was 54.3%. Analysing Y_r for systems A and B, it is important to highlight that a high probability occurs that the simulated H_i estimated using Meteonorm 8.0 in PVsyst is less accurate for both case studies conducted.

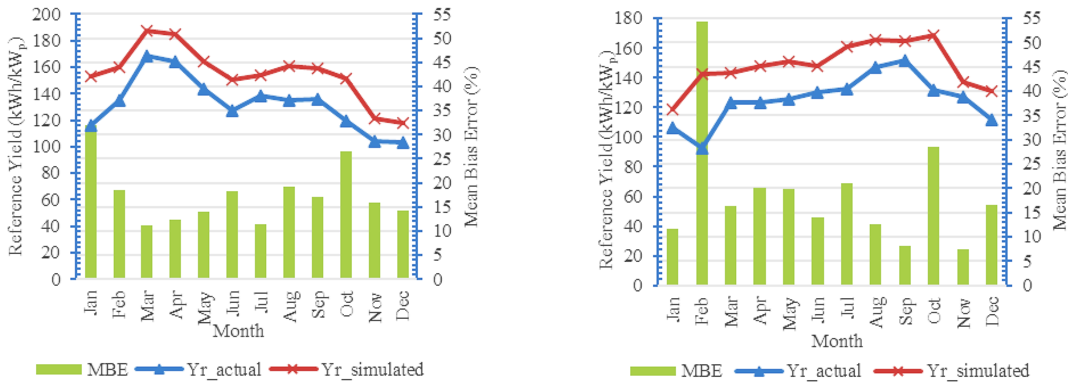

(a) (b)

Figure 6. Comparison between the actual reference yield (Y_{r_actual}) with the simulated reference yield $Y_{r\_simulated}$) for (a) system A and (b) system B

3.2.3. Final yield

Figure 7(a) shows the comparison of the monthly actual final yield (Y_{f_actual}) and simulated final yield ($Y_{f\_simulated}$)combined with the corresponding MBE for system A. The figure shows that the trends of the actual and simulated E_{out} are almost similar, with slight variations in January. The highest Y_{f_actual} was recorded in March with a value of 142.0 kWh/kW$_p$, while the lowest Y_{f_actual} was recorded in December with a value of 90.1 kWh/kW$_p$. The figure shows that $Y_{f\_simulated}$ predicted acceptable values for the entire year ranging from -0.3% to 10.9%. Nevertheless, note that the MBE in January was quite high, which was 10.9% that indicates the actual value is much lower than the simulated value.

Figure 7(b) shows the comparison of monthly Y_{f_actual} and $Y_{f\_simulated}$ combined with the corresponding MBE for system B. The actual and simulated E_{out} trends show that they are not in good agreement, except for the three months, that is, January, September, and November. The highest Y_{f_actual} was recorded in September, which was 119.5 kWh/kW$_p$, while the lowest was recorded in February, with a value of 79.3 kWh/kW$_p$. Fundamentally, Y_f was directly proportional to the value of E_{out} produced in the same month [7]. Therefore, the higher the H_{i_actual}, the higher is the E_{out_actual} and consequently, the higher is the Y_{f_actual} obtained. The figure also shows that the $Y_{f\_simulated}$ was overestimated for the entire year. The MBE varied in the range of -0.2% to 34%. The highest MBE was in February, which was -33.9%.

3.2.4. Performance ratio

Figure 8(a) shows the comparison of the monthly actual performance ratio ($PR_{\_actual}$) and simulated performance ratio ($PR_{\_simulated}$) combined with the corresponding MBE for system A. The figure shows that the actual and simulated PR, trends were in good agreement with each other. The range of $PR_{\_actual}$ was

84% to 89%, while the range of simulated PR, was 72% to 74%. The highest $PR_{\_actual}$ of 89% was obtained in October and the lowest $PR_{\_actual}$ was in March at 84.1%. The MBE was in the range of -14% to -18%, which was in good agreement with a previous study conducted in the same climate region reported by Anang *et al*. [7], which was 15% to 16% 7.

The highest MBE was attained in October, which was 18%. Because the highest Y_{f_actual} was recorded in March, it was expected that March will obtain the highest PR. Interestingly, the results showed that October was the month in which the GCPV system obtained the highest PR,, which indicates that Y_{f_actual} is not the parameter that solely affects the PR value, as stated in a previous study [43]. The reason for the lowest PR value could be thermal losses, considering that March had the highest H_{i_actual} value of 168.8 kWh/m^2 [23]. The average module temperature during the operation in the year 2019 ranged between 25℃ and 67℃, and the average temperature of the PV module in March was 42 ℃. Thus, it contributes significantly to the thermal losses experienced by system A.

Figure 8(b) shows a monthly comparison of $PR_{\_actual}$ and $PR_{\_simulated}$ combined with the corresponding MBE for system B. The figure also shows that the actual and simulated PR, trends were in good agreement with each other. The range of $PR_{\_actual}$ for system B lied between 77% and 86%, while the $PR_{\_simulated}$ ranged 74% to 75%. The highest $PR_{\_actual}$ was at 85.70% in February and the lowest $PR_{\_actual}$ was in December at 77.24%. The figure also shows that $PR_{\_simulated}$ was lower than $PR_{\_actual}$. The MBE ranged from -3% to -13%. The highest MBE was in February, which was 13.1%. PVsyst underpredicted the value of $PR_{\_simulated}$ for the entire year in 2020. This may be because the of the overestimated value of the losses inserted into the PVsyst simulation. The value of the losses used was based on the worst-case scenario. Therefore, $PR_{\_simulated}$ is lower than $PR_{\_actual}$ for system B.

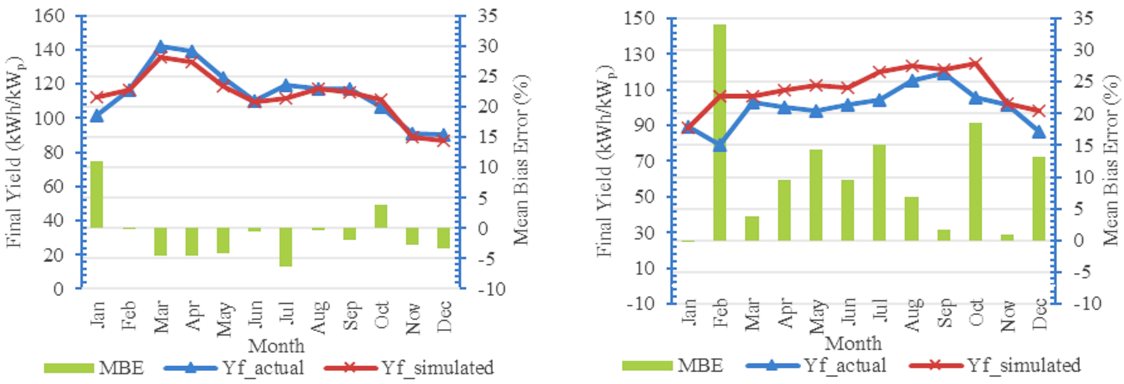

(a) (b)

Figure 7. Comparison between the actual final yield (Y_{f_actual}) with the simulated final yield ($Y_{f\_simulated}$) for (a) system A and (b) system B

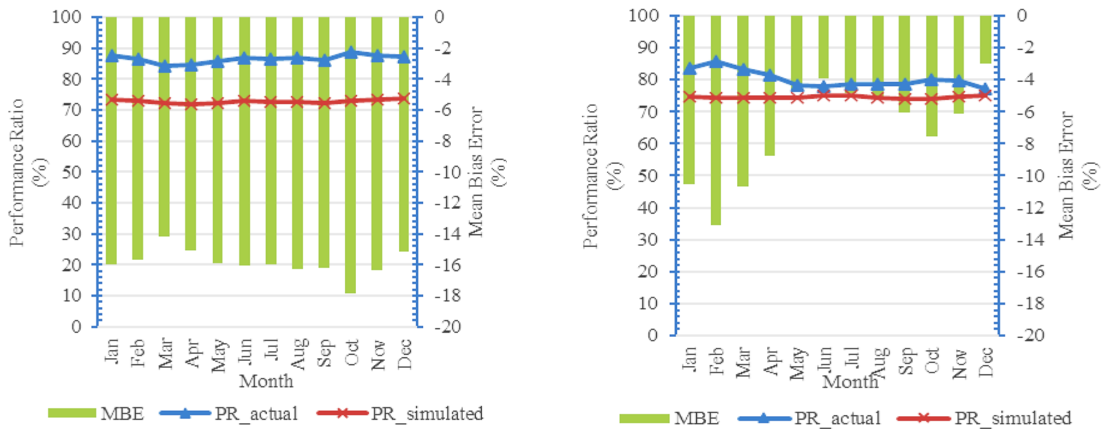

(a) (b)

Figure 8. Comparison between the actual performance ratio ($PR_{\_actual}$) and simulated performance ratio ($PR_{\_simulated}$) for (a) system A and (b) system B

3.2.5. Annual capacity factor (CF)

The actual annual capacity factor CF_{actual} obtained in this study for system A was 15.7%, whereas the simulated capacity factor $CF_{simulated}$ calculated from the simulation results with the Meteonorm-derived long-term average values was 15.5%. The MBE for the CF value was very small, 1.4%. The annual CF_{actual} obtained in this study for system B was 13.8%, whereas the $CF_{simulated}$ was 15.4%, with an MBE of 10.1%. Because the value of CF is strongly dependent on the value of E_{out} recorded, as in (4), the results follow as the equation perceives.

In summary, the ranges of the monthly actual and simulated technical performance are listed in Table 5. The table notably shows that for system A, PVsyst overpredicted the value of the H_i and Y_f in the range of approximately 11% to 32% but underpredicted the PR, by 15% to 18%. Similarly, for system B, PVsyst also overpredicted the value of the H_i and Y_f but in a bigger range of approximately 8% to 54 % and underpredicted the value of PR approximately 4% to 11%.

Referring to Table 6, the yearly values of the simulated E_{out}, Y_r, Y_f, PR, and CF for system A were 7.38 MWh, 1864.25 kWh/kW$_p$, 1355.59 kWh/kW$_p$, 72.8%, and 15.5%, respectively. In contrast, the actual yearly values of measured E_{out}, Y_r, Y_f, PR, and CF were 7.40 MWh, 1591.6 kWh/kW$_p$, 1374.7 kWh/kW$_p$, 86.5% and 15.7%, respectively. The MBE for the E_{out}, Y_r, Y_f, PR, and CF was -0.4%, 17.1%, -1.4%, -15.0%, and 1.4% respectively.

For system B, the yearly values of simulated E_{out}, Y_r, Y_f, PR, and CF were 242.7 MWh, 1779.7 kWh/kW$_p$, 1325.43 kWh/kW$_p$, 74.5%, and 15.1%, respectively. In contrast, the actual yearly values of the measured E_{out}, Y_r, Y_f, PR, and CF were 221.1 MWh, 1504.1 kWh/kW$_p$, 1204.1 kWh/kW$_p$, 80.3%, and 13.8%, respectively. The MBE for E_{out}, Y_r, Y_f, PR, and CF was 9.80%, 18.3%, 10.0%, -7.2% and 10.0%, respectively.

When comparing the monthly MBE with the yearly MBE of the technical performances for systems A and B, a larger deviation is observed for the monthly values compared to the yearly values. In the yearly overall analysis, unfavorable predictions in certain periods of the year may be masked by overestimations balancing out underestimations, as demonstrated in a prior study by Gonzalez-Pena [44] which found a smaller annual deviation ranging from 1% to 15%.

Table 5. Range of monthly actual and simulated technical performance

		Range of monthly technical performance				
		H_i (kWh/m^2)	E_{out} (kWh)	Y_r (kWh/kW$_p$)	Y_f (kWh/kW$_p$)	PR (%)
System A	Actual	103.4 to 168.8	485.2 to 765.3	103.4 to 168.8	90.0 to 142.0	84.1 to 89.0
	Simulated	118.0 to 187.6	474.6 to 737.2	118.1 to 187.6	87.1 to 135.5	72.0 to 74.0
MBE (%)		11.1 to 32.0	-0.4 to 11.9	11.1 to 32.0	-0.3 to 10.9	-15.0 to -18.0
System B	Actual	92.5 to 152.0	14550.6 to 21948.0	92.5 to 152.0	79.3 to 119.5	77.2 to 85.7
	Simulated	119.0 to 168.8	16329.0 to 22957.0	119.0 to 169.0	89.0 to 125.0	74.1 to 74.9
MBE (%)		7.6 to 48.9	-0.2 to 29.4	7.5 to 54.3	-0.2 to 34.0	-3.9 to -10.5

Table 6. Yearly actual and simulated technical performance

		Yearly technical performance				
		E_{out} (MWh)	Y_r (kWh/kW$_p$)	Y_f (kWh/kW$_p$)	PR (%)	CF (%)
System A	Actual	7.40	1591.6	1374.7	86.5	15.7
	Simulated	7.38	1864.3	1355.6	72.8	15.5
MBE (%)		-0.4	17.1	-1.4	-15.8	-1.4
System B	Actual	221.1	1504.1	1204.1	80.3	13.8
	Simulated	242.7	1779.7	1325.4	74.5	15.1
MBE (%)		9.8	18.3	10.0	-7.2	10.0

3.3. Comparison of the actual technical performance of system A and B with other studies

In order to have the element of comparison, this section addresses the actual technical performance of systems A and B together with performances from other studies. The technical performance parameters of Y_f, PR, and CF obtained in both systems; system A and B in this study, are found to be in the value range of the several studies as in Table 7. However, it is worthy to notify that both systems in this study have slightly lower CF when compared to the value of CF in tropical climates obtained by J. Ascencio-Vásquez, where the CF s ranged between 16% and 18% [45]. Despite the high irradiation levels in the tropical climate, the CF is lower than in other areas with high irradiation values owing to the year-round tropical rain, cloud cover, and constant high ambient temperature [45].

Table 7. Technical performance of the previous studies including the present study

No	Author	Location	Climate	Capacity (kW)	Yearly technical performance				
					E_{out} (MWh)	Y_r (kWh/kW$_p$)	Y_f (kWh/kW$_p$)	PR (%)	CF (%)
1	[7]	Malaysia	Af	7.8	9.4	-	1204.5	65.0	13.7
				7.8	10.7	-	1379.7	71.0	15.7
2	[20]	Malaysia	Af	619.0	0.9	-	-	77.0	12
3	[46]	Louisiana	Cfa	1100.0	-	-	1277.5	73.0	14.8
4	[47]	Malawi	Cfa	830.0	-	-	1551.2	79.5	17.7
5	[48]	Malaysia	Af	18.0	9.9	-	1579.0	91.5	18
				18.0	8.9	-	1520.0	83.7	17.4
				18.0	8.9	-	1452.0	80.0	16.6
6	[49]	Ghana	Aw	2500.0	3547.0	-	-	70.4	16.2
7	[50]	Thailand	Af	3.5	-	-	1387.0	76.4	-
8	[51]	Singapore	Af	142.5	-	-	1138.0	81.0	-
9	[52]	Malaysia	Af	5.8	0.02	-	949.0	63.6	-
10	Present study	Malaysia	Af	5.4	7.4	1591.6	1374.7	86.5	15.7
11	Present Study	Indonesia	Af	183.6	221.1	1504.1	1204.1	80.3	13.8

Legend: Cfa: Humid subtropical climate, Aw: Tropical Savanna Climate, Af: tropical rainforest climate

4. CONCLUSION

The study uniquely presented the performances from two GCPV systems located at opposites latitudes from the equatorial line; a 5.39 kW$_p$ free-standing GCPV system installed in Kelantan, Malaysia (northern latitude-system A), and a 183.6 kW$_p$ rooftop GCPV system installed in Cikarang, Indonesia (southern latitude-system B), which was monitored during 2019 and 2020, respectively. The study succeeded in comparing the simulated and actual technical performances of both systems. The following summaries and conclusions were drawn: i) For system A, the yearly values of simulated E_{out}, Y_r, Y_f, PR, and CF were 7.38 MWh,1864.25 kWh/kW$_p$, 1355.59 kWh/kW$_p$,72.8%, and 15.5%, respectively; ii) In contrast, the actual yearly values of measured E_{out}, Y_r, Y_f, PR, and CF were 7.40 MWh, 1591.6 kWh/kW$_p$, 1374.7 kWh/kW$_p$, 86.5%, and 15.7%, respectively; iii) The MBE for the E_{out}, Y_r, Y_f, PR, and CF was -0.4%, 17.1%, -1.4%, -15.8%, and 1.4%, respectively; iv) For system B, the yearly values of simulated E_{out}, Y_r, Y_f, PR, and CF were 242.7 MWh, 1779.7 kWh/kW$_p$, 1325.43 kWh/kW$_p$, 74.5%, and 15.1%, respectively; v) In contrast, the actual yearly values of measured E_{out}, Y_r, Y_f, PR, and CF were 221.1 MWh, 1504.1 kWh/kW$_p$, 1204.1 kWh/kW$_p$, 80.3%, and 13.8%, respectively; vi) The MBE for the E_{out}, Y_r, Y_f, PR, and CF was 9.80%, 18.3%, 10.0%, -7.2%, and 10.0%, respectively; vii) This study demonstrates that the most significant inaccuracy in the simulated technical performance was resulted from the value of irradiation imported into the PVsyst using Meteonorm 8.0; viii) Because E_{out}, Y_f, and PR, are related to the amount of H_i, some deviation occurs between the simulated and actual technical performance; and ix) While some difference exists between the technical performance of system A in the northern hemisphere and its simulated results, they are notably more consistent with each other than that in system B, in the southern hemisphere.

ACKNOWLEDGEMENTS

The authors express gratitude to the owner of the GCPV systems and Solar Photovoltaic Energy Conversion Technology and Research Application (SPECTRA) group for their valuable inputs, Strategic Research Partnering (SRP) research grant 100-RMC 5/3/SRP (034/2021), and the Bilateral Strategic Alliance (UI-UITM BISA) NKB676/UN2. RST/HKP.05.00/2021 research grant, to funding this research.

REFERENCES

[1] P. Narkwatchara, C. Ratanatamskul, and A. Chandrachai, "Performance analysis of electricity generation from grid-connected photovoltaic system using All-Sky Index for Smart City projects in Thailand," *Renewable Energy*, vol. 171, pp. 315–327, Jun. 2021, doi: 10.1016/j.renene.2021.02.107.

[2] Renewables Now, "Renewables 2021 Global Status Report," 2021. [Online]. Available: https://www.ren21.net/wp-content/uploads/2019/05/GSR2021_Full_Report.pdf

[3] IEA, "IEA PVPS ANNUAL REPORT 2020 PHOTOVOLTAIC POWER SYSTEMS PROGRAMME," 2021. [Online]. Available: https://iea-pvps.org/wp-content/uploads/2021/04/IEA-PVPS-AR-2020.pdf

[4] D. B. Magare *et al.*, "Effect of seasonal spectral variations on performance of three different photovoltaic technologies in India," *International Journal of Energy and Environmental Engineering*, vol. 7, no. 1, pp. 93–103, Mar. 2016, doi: 10.1007/s40095-015-0190-0.

[5] K. Padmavathi and S. A. Daniel, "Performance analysis of a 3MWp grid connected solar photovoltaic power plant in India," *Energy for Sustainable Development*, vol. 17, no. 6, pp. 615–625, Dec. 2013, doi: 10.1016/j.esd.2013.09.002.

[6] A. Necaibia *et al.*, "Analytical assessment of the outdoor performance and efficiency of grid-tied photovoltaic system under hot dry climate in the south of Algeria," *Energy Conversion and Management*, vol. 171, pp. 778–786, Sep. 2018, doi:

10.1016/j.enconman.2018.06.020.
[7] N. Anang, S. N. A. Syd Nur Azman, W. M. W. Muda, A. N. Dagang, and M. Z. Daud, "Performance analysis of a grid-connected rooftop solar PV system in Kuala Terengganu, Malaysia," *Energy and Buildings*, vol. 248, p. 111182, Oct. 2021, doi: 10.1016/j.enbuild.2021.111182.
[8] D. H. Daher, L. Gaillard, M. Amara, and C. Ménézo, "Impact of tropical desert maritime climate on the performance of a PV grid-connected power plant," *Renewable Energy*, vol. 125, pp. 729–737, Sep. 2018, doi: 10.1016/j.renene.2018.03.013.
[9] L. C. Lima, L. A. Ferreira, and F. H. B. L. Morais, "Performance analysis of a grid connected photovoltaic system in northeastern Brazil," *Energy for Sustainable Development*, vol. 37, pp. 79–85, 2016.
[10] M. CACERES, A. BUSSO, L. VERA, and A. FIRMAN, "Primer Sistema Fotovoltaico Conectado a La Red De Baja Tensión Del Norte Argentino: Caracterización Y Analisis," *Dyna Energia Y Sostenibilidad*, vol. 6, no. 1, p. [13 p.]-[13 p.], 2017, doi: 10.6036/es8151.
[11] M. Mpholo, T. Nchaba, and M. Monese, "Yield and performance analysis of the first grid-connected solar farm at Moshoeshoe I International Airport, Lesotho," *Renewable Energy*, vol. 81, pp. 845–852, Sep. 2015, doi: 10.1016/j.renene.2015.04.001.
[12] P. Tozzi and J. H. Jo, "A comparative analysis of renewable energy simulation tools: Performance simulation model vs. system optimization," *Renewable and Sustainable Energy Reviews*, vol. 80, pp. 390–398, Dec. 2017, doi: 10.1016/j.rser.2017.05.153.
[13] A. A. F. Husain, M. H. A. Phesal, M. Z. A. A. Kadir, U. A. U. Amirulddin, and A. H. J. Junaidi, "A decade of transitioning malaysia toward a high-solar pv energy penetration nation," *Sustainability (Switzerland)*, vol. 13, no. 17, 2021, doi: 10.3390/su13179959.
[14] J. L. D. S. Silva, T. S. Costa, K. B. De Melo, E. Y. Sako, H. S. Moreira, and M. G. Villalva, "A comparative performance of PV power simulation software with an installed PV plant," in *Proceedings of the IEEE International Conference on Industrial Technology*, 2020, vol. 2020-Febru, pp. 531–535. doi: 10.1109/ICIT45562.2020.9067138.
[15] E. Tarigan, Djuwari, and F. D. Kartikasari, "Techno-economic simulation of a grid-connected PV system design as specifically applied to residential in Surabaya, Indonesia," *Energy Procedia*, vol. 65, pp. 90–99, 2015, doi: 10.1016/j.egypro.2015.01.038.
[16] A. Z. Abdullah, M. H. Amlus, N. Azizan, I. M. Sali, and M. H. Rahim, "Performance analysis of different Type PV module for 3kW residential roof top PV system using PVSyst simulation tool," *Journal of Physics: Conference Series*, vol. 2312, no. 1, p. 012042, Aug. 2022, doi: 10.1088/1742-6596/2312/1/012042.
[17] T. M. N. T. Mansur, N. H. Baharudin, and R. Ali, "Performance analysis of self-consumed solar PV system for a fully DC residential house," *Indonesian Journal of Electrical Engineering and Computer Science*, vol. 8, no. 2, pp. 391–398, Nov. 2017, doi: 10.11591/ijeecs.v8.i2.pp391-398.
[18] A. A. F. Husain, M. H. A. Phesal, M. Z. A. Ab Kadir, and U. A. Ungku Amirulddin, "Techno-economic analysis of commercial size grid-connected rooftop solar pv systems in malaysia under the nem 3.0 scheme," *Applied Sciences (Switzerland)*, vol. 11, no. 21, p. 10118, Oct. 2021, doi: 10.3390/app112110118.
[19] PVsyst SA, "PVsyst Help Contents." https://www.pvsyst.com/help/index.html?contents_table.htm (accessed Sep. 27, 2023).
[20] M. N. Raj and J. Pasupuleti, "Performance assessment of a 619kW photovoltaic power plant in the northeast of peninsular Malaysia," *Indonesian Journal of Electrical Engineering and Computer Science*, vol. 20, no. 1, pp. 9–15, 2020, doi: 10.11591/ijeecs.v20.i1.pp9-15.
[21] Y. Siregar, Y. Hutahuruk, and Suherman, "Optimization design and simulating solar PV system using PVSyst software," in *2020 4th International Conference on Electrical, Telecommunication and Computer Engineering, ELTICOM 2020 - Proceedings*, 2020, pp. 219–223. doi: 10.1109/ELTICOM50775.2020.9230474.
[22] D. Okello, E. E. Van Dyk, and F. J. Vorster, "Analysis of measured and simulated performance data of a 3.2 kWp grid-connected PV system in Port Elizabeth, South Africa," *Energy Conversion and Management*, vol. 100, pp. 10–15, Aug. 2015, doi: 10.1016/j.enconman.2015.04.064.
[23] H. Vidal, M. Rivera, P. Wheeler, and N. Vicencio, "The analysis performance of a grid-connected 8.2 kwp photovoltaic system in the patagonia region," *Sustainability (Switzerland)*, vol. 12, no. 21, pp. 1–16, Nov. 2020, doi: 10.3390/su12219227.
[24] S. Goel and R. Sharma, "Analysis of measured and simulated performance of a grid-connected PV system in eastern India," *Environment, Development and Sustainability*, vol. 23, no. 1, pp. 451–476, Jan. 2021, doi: 10.1007/s10668-020-00591-7.
[25] R. E. Izzaty, B. Astuti, and N. Cholimah, "Seda Malaysia Grid-Connected Photovoltaic Systems Design Course," in *Angewandte Chemie International Edition, 6(11), 951–952.*, 1967, pp. 5–24.
[26] M. Z. Hussin, A. M. Omar, Z. Md Zain, S. Shaari, and H. Zainuddin, "Design Impact of 6.08 kWp Grid-Connected Photovoltaic System at Malaysia Green Technology Corporation," *International Journal of Electrical and Electronic Systems Research*, vol. 5, 2012.
[27] H. Zainuddin, S. Shaari, A. M. Omar, Z. M. Zain, J. Soumin, and Z. Surat, "Preliminary investigations on the effect of humidity on the reception of visible solar radiation and the effect of humidity and wind speed on PV module output," *AIP Conference Proceedings*, vol. 1250, pp. 55–58, 2010, doi: 10.1063/1.3469733.
[28] B. Marion *et al.*, "Performance parameters for grid-connected PV systems," in *Conference Record of the Thirty-first IEEE Photovoltaic Specialists Conference, 2005.*, 2005, pp. 1601–1606. doi: 10.1109/PVSC.2005.1488451.
[29] F. A. M. Shukor, H. Zainuddin, N. Muhammad, and F. L. M. Khir, "Acceptance ratio analysis: An early fault indicator for grid-connected photovoltaic system," *International Journal on Advanced Science, Engineering and Information Technology*, vol. 11, no. 3, p. 1214, Jun. 2021, doi: 10.18517/ijaseit.11.3.12614.
[30] M. M. Muhamad Hanifah, "Determination of nominal operating cell temperature for photovoltaic modules in tropical Malaysia," Universiti Teknologi MARA, 2020.
[31] M. Z. Hussin, N. D. M. Sin, H. Zainuddin, A. M. Omar, and S. Shaari, "Anomaly detection of grid connected photovoltaic system based on degradation rate: A case study in Malaysia," *Pertanika Journal of Science and Technology*, vol. 29, no. 4, pp. 3143–3159, Oct. 2021, doi: 10.47836/PJST.29.4.48.
[32] G. Abdullah and H. Nishimura, "Techno-economic performance analysis of a 40.1 kWp grid-connected photovoltaic (GCPV) system after eight years of energy generation: A case study for Tochigi, Japan," *Sustainability (Switzerland)*, vol. 13, no. 14, 2021, doi: 10.3390/su13147680.
[33] Department of Standards Malaysia, "Installation of grid-connected photovoltaic (PV) system (Second revision)," 2018. https://mysol.jsm.gov.my/getPdfFile/eyJpdiI6InhiaStma2JDUFNqcUJwNkFXT2JGYUE9PSIsInZhbHVlIjoiT3ZKaUVEMXhuOFpkWWVtbTFYM0gxUT09IiwibWFjIjoiM2NjMWViNjY1ODkwYWE4MTBhOGRkOGMyYzllZWJlZjIxY2ZhMmQzZTdjMTYzZmNiNTZmYTRlNDA3ZGU1NjM2NSJ9
[34] A. Allouhi, R. Saadani, M. S. Buker, T. Kousksou, A. Jamil, and M. Rahmoune, "Energetic, economic and environmental (3E) analyses and LCOE estimation of three technologies of PV grid-connected systems under different climates," *Solar Energy*, vol. 178, pp. 25–36, Jan. 2019, doi: 10.1016/j.solener.2018.11.060.
[35] I. Baghdadi, A. El Yaakoubi, K. Attari, Z. Leemrani, and A. Asselman, "Performance investigation of a PV system connected to the grid," *Procedia Manufacturing*, vol. 22, pp. 667–674, 2018, doi: 10.1016/j.promfg.2018.03.096.

[36] A. Elkholy, F. H. Fahmy, A. A. Abou El-Ela, A. E.-S. A. Nafeh, and S. R. Spea, "Experimental evaluation of 8kW grid-connected photovoltaic system in Egypt," *Journal of Electrical Systems and Information Technology*, vol. 3, no. 2, pp. 217–229, Sep. 2016, doi: 10.1016/j.jesit.2015.10.004.
[37] R. Sharma and S. Goel, "Performance analysis of a 11.2 kWp roof top grid-connected PV system in Eastern India," *Energy Reports*, vol. 3, pp. 76–84, Nov. 2017, doi: 10.1016/j.egyr.2017.05.001.
[38] M. A. Omar and M. M. Mahmoud, "Grid connected PV- home systems in Palestine: A review on technical performance, effects and economic feasibility," *Renewable and Sustainable Energy Reviews*, vol. 82, pp. 2490–2497, Feb. 2018, doi: 10.1016/j.rser.2017.09.008.
[39] International Electrotechnical Commission, "Photovoltaic system performance-Part 1: Monitoring," 2021.
[40] M. Malvoni, A. Leggieri, G. Maggiotto, P. M. Congedo, and M. G. De Giorgi, "Long term performance, losses and efficiency analysis of a 960 kWP photovoltaic system in the Mediterranean climate," *Energy Conversion and Management*, vol. 145, pp. 169–181, 2017, doi: 10.1016/j.enconman.2017.04.075.
[41] K. C. Tan, "Trends of rainfall regime in Peninsular Malaysia during northeast and southwest monsoons," *Journal of Physics: Conference Series*, vol. 995, no. 1, p. 012122, Apr. 2018, doi: 10.1088/1742-6596/995/1/012122.
[42] S. Thotakura *et al.*, "Operational performance of megawatt-scale grid integrated rooftop solar PV system in tropical wet and dry climates of India," *Case Studies in Thermal Engineering*, vol. 18, 2020, doi: 10.1016/j.csite.2020.100602.
[43] N. Umar, B. S. Panwar, B. Bora, and C. Banerjee, "Comparison of Different PV Power Simulation Softwares: Case Study on Performance Analysis of 1 MW Grid-Connected PV Solar Power Plant," *International Journal of Engineering Science Invention (IJESI)*, vol. 7, no. 7, pp. 11–24, 2018.
[44] D. González-Peña, I. García-Ruiz, M. Díez-Mediavilla, M. I. Dieste-Velasco, and C. Alonso-Tristán, "Photovoltaic prediction software: Evaluation with real data from northern Spain," *Applied Sciences (Switzerland)*, vol. 11, no. 11, 2021, doi: 10.3390/app11115025.
[45] J. Ascencio-Vásquez, K. Brecl, and M. Topič, "Methodology of Köppen-Geiger-Photovoltaic climate classification and implications to worldwide mapping of PV system performance," *Solar Energy*, vol. 191, pp. 672–685, Oct. 2019, doi: 10.1016/j.solener.2019.08.072.
[46] D. J. Veerendra Kumar *et al.*, "Performance Evaluation of 1.1 MW Grid-Connected Solar Photovoltaic Power Plant in Louisiana," *Energies*, vol. 15, no. 9, 2022, doi: 10.3390/en15093420.
[47] M. H. Banda, K. Nyeinga, and D. Okello, "Performance evaluation of 830 kWp grid-connected photovoltaic power plant at Kamuzu International Airport-Malawi," *Energy for Sustainable Development*, vol. 51, pp. 50–55, 2019, doi: 10.1016/j.esd.2019.05.005.
[48] H. S. Mohammed, C. K. Gan, and K. A. Baharin, "Performance Evaluation of Various Solar Photovoltaic Module Technologies under Tropical Climate Conditions at Melaka, Malaysia," *ARPN Journal of Engineering and Applied Sciences*, vol. 14, no. 2, pp. 336–341, Dec. 2019, doi: 10.36478/JEASCI.2019.336.341.
[49] L. D. Mensah, J. O. Yamoah, and M. S. Adaramola, "Performance evaluation of a utility-scale grid-tied solar photovoltaic (PV) installation in Ghana," *Energy for Sustainable Development*, vol. 48, pp. 82–87, Feb. 2019, doi: 10.1016/j.esd.2018.11.003.
[50] A. Chaita and J. Kluabwang, "Performance evaluation of 3.5 kWp rooftop solar PV plant in Thailand," *Lecture Notes in Engineering and Computer Science*, vol. 2, pp. 572–575, 2016.
[51] S. Wittkopf, S. Valliappan, L. Liu, K. S. Ang, and S. C. J. Cheng, "Analytical performance monitoring of a 142.5kW p grid-connected rooftop BIPV system in Singapore," *Renewable Energy*, vol. 47, pp. 9–20, 2012, doi: 10.1016/j.renene.2012.03.034.
[52] K. Sopian, S. Shaari, N. Amin, and R. Zulkifli, "Performance of a grid-connected photovoltaic system in Malaysia Solar Dryer Systems View project Techno-Economical Assessment of Photovoltaic Systems View project Kamaruzzaman Bin Sopian," *Article in International Journal of Engineering and Technology*, 2007.

BIOGRAPHIES OF AUTHORS

Yang Ilya Akila Abdul Rahim is currently a master student in Applied Physic Department at the Universiti Teknologi Mara (UiTM), Shah Alam, with supervision of Associate Professor Dr Hedzlin Zainuddin. She receives her bachelor's in physics (Hons) from UiTM in 2021. Her undergraduate thesis focused on comparison between SEDA's standalone photovoltaic design model and PVsyst SAPV design simulation software and now is conducting analysis on the performance of the photovoltaic system in tropical region. She can be contacted at email: yangilyaakila@gmail.com.

Hedzlin Zainuddin received her B. Sc in Physics from Universiti Kebangsaan Malaysia in the year 2000. She obtained her M. Sc in Photovoltaics Energy System from the same university in the year 2003. In 2014, she completed her Ph. D in photovoltaics from Universiti Teknologi MARA, Shah Alam, Malaysia. Her specialization areas are physics, solar photovoltaic (PV) field testing, design of grid-connected PV (GCPV) system, design of off-grid PV (OGPV) system, mathematical and computational modeling (linear, multiple linear and artificial intelligent) and PV system fault detection. She presently holds four certificates of competency in GCPV and OGPV. She has been working with Industries and Government Agencies for 13 years since 2007 through consultation projects. She can be contacted at email: hedzl506@uitm.edu.my.

Eko Adhi Setiawan got PhD in Institut für Solare Energieversorgungstechnik - ISET Kassel, Germany, 2007. He was director of Tropical Renewable Energy Center (TREC) and Head of Energy System Engineering master's degree Program - Faculty of Engineering Universitas Indonesia. His focus research is renewable energy integration, developing concept of dual power AC and DC Voltage in the house, for more independent, near zero export and import power with the utility grids. He was a project leader in many renewable energy research and implementation such as developing of 1st bifacial floating PV in Indonesia with industry partners, developing power converter for household appliances application (LPDP grant 2010-2022), research development, and commissioning of three units of 3 kW converter for DC microgrids at HNEI (Hawai'i Natural Energy Institute 2021). He was energy Coordinator for New Capital City – IKN Transition Team, Republic of Indonesia. He can be contacted at email: ekoas@eng.ui.ac.id.

Alfian Ferdiansyah Madsuha finished his Ph.D. at Albert-Ludwigs University of Freiburg, Germany, in 2017. His research is focused on the solar cell, nanomaterial, and renewable energy. Currently, he is a researcher in Tropical Renewable Energy Center (TREC), in the Faculty of Engineering, Universitas Indonesia. He is an assistant professor in the Department of Metallurgical and Materials Engineering, Universitas Indonesia. He has a research interest in solar cell / photovoltaic from lab scale to industrial. He can be contacted at email: alfian@eng.ui.ac.id.

Mohamad Zhafran Hussin obtained his Bachelor of Electrical (Hons) Engineering from UiTM Shah Alam. Currently, he serves as a senior lecturer at UiTM Cawangan Johor Kampus Pasir Gudang in Power Department. His main research interests are Renewable Energy (RE), Energy efficiency (EE) and Electrical Machines. He can be contacted at email: mzhafran@uitm.edu.my.

Shahril Irwan Sulaiman holds a PhD in Electrical Engineering from Universiti Teknologi MARA, Malaysia. He obtained his M.EngSc in Photovoltaic Engineering from University of New South Wales, Australia, and B.Eng in Electrical & Electronics from Universiti Tenaga Nasional, Malaysia. He is currently a senior lecturer in Faculty of Electrical Engineering, Universiti Teknologi MARA, Malaysia. His active contributions have been recognized when he is appointed as one of the Master Trainers by Sustainable Energy Development Authority (SEDA) Malaysia to conduct competency-based trainings related to design, installation, testing & commissioning, operation and maintenance of both grid-connected photovoltaic systems and stand-alone photovoltaic systems. He can be contacted at email: shahril_irwan2004@yahoo.com.

Siti Nor Nadhirah Ibrahim is a student in Faculty of Applied Science at the Universiti Teknologi MARA (UiTM), Shah Alam, Selangor, Malaysia. She received her B.Sc. degree with honours in Industrial Physics from UiTM Shah Alam in 2022. Currently, she is a research assistant under the Strategic Research Partnership (SRP) supervised by Associate Professor Dr. Hedzlin Zainuddin. For her final year project, she conducted research on electrical properties of nc-SiC synthesized by hot wire chemical vapour deposition method. She can be contacted at email: sitinornadhirahibrahim251@gmail.com.